Topological protected quantum critical point in 1D Two Impurity Models

Benedikt Lechtenberg,[1] Fabian Eickhoff,[1] and Frithjof B. Anders[1]

[1] *Lehrstuhl für Theoretische Physik II, Technische Universität Dortmund, 44221 Dortmund,Germany*

(Dated: October 3, 2016)

We show that the two impurity Anderson model exhibit an additional quantum critical point at infinitely many specific distances between both impurities for an inversion symmetric 1D dispersion. Unlike the quantum critical point previously established by Jones and Varma, it is robust against particle-hole or parity symmetry breaking. The quantum critical point separates a spin doublet from a spin singlet ground state and is, therefore, topological protected. A finite single particle tunneling t or an applied uniform gate voltages will drive the system across the quantum critical point. The discriminative magnetic properties of the different phases cause a jump in the spectral functions at low temperature which might be useful for future spintronics devices. A local parity conservation will prevent the spin-spin correlation function to decay to its equilibrium value after spin-manipulations.

PACS numbers: 03.65.Yz, 73.21.La, 73.63.Kv, 76.20.+q

arXiv:1609.09750v1 [cond-mat.str-el] 30 Sep 2016

Introduction.– The promising perspective of combining traditional electronics with novel spintronics devices leads to an intense research of controlling and switching magnetic properties of such nano-devices. Experimentally magnetic properties of adatoms one surfaces [1–5] or magnetic molecules [6–12] might serve as smallest building blocks for spintronic devices. From a theoretical perspective, the two impurity Anderson model (TIAM) [13] constitute an important but simple system which embodies the competition of interactions between two localized magnetic moments with those between the impurities and the conduction band.

A well known quantum critical point (QCP) was predicted for the TIAM [13, 14] separating a singlet phase where both impurity spins are bound into a local singlet for strong antiferromagnetic interactions between the impurities and another singlet phase where both impurity spins are completely screened by the conduction band. This QCP [14] turned out to be unstable against particle-hole (PH) symmetry breaking [15] and is a consequence of unphysical approximations [16]. It is generically replaced by a crossover regime [17–19] that can be broad.

In this letter we establish that the model exhibit another stable QCP for any inversion symmetric 1D dispersion depending only on the absolute value of the wave vector. The existence of this different QCP relies only on the fact that for specific distances R between both impurities either the even or odd parity contributions to the conduction band decouples from the impurities at low energy scales leading to an underscreened Kondo effect. This underscreened Kondo fixed point (USK FP) [20] has a doublet ground state which is topological different to the singlet ground state for large antiferromagnetic interactions between both impurities excluding a smooth crossover between both phases. This QCP also exist for the limit $R \to 0$ in all dimensions [21, 22]: For this special case the QCP has been recently observed in molecular dimers [6] where the different phases can clearly be detected in the scanning tunneling spectra.

Here, we present the generalization to finite distances, its robustness against particle-hole symmetry as well as parity breaking and demonstrate that the quantum phase transition (QPT) can also be evoked by applying a gate voltage to the impurities. Since the entanglement between the impurity spins is protected by a dynamical symmetry in the parity-symmetric case, the spin-spin correlation function cannot completely decay to its equilibrium value, and, therefore, might be useful for future qubit implementations.

Possible experimental realizations for finite distances could be in pseudo 1D nano structures [23–27] or optical lattices [28–30].

Model.– We consider the two impurity Anderson model (TIAM) whose Hamiltonian can be separated into the parts $H_{\rm TIAM} = H_{\rm c} + H_{\rm D} + H_{\rm I}$. $H_{\rm c}$ contains the conduction band $H_{\rm c} = \sum_{\vec{k},\sigma} \epsilon(\vec{k}) c^\dagger_{\vec{k},\sigma} c_{\vec{k},\sigma}$ and $H_{\rm D}$ and $H_{\rm I}$ comprise the impurity contribution and the interaction between the conduction band and impurities respectively

$$H_{\rm D} = \sum_{j,\sigma} E_j d^\dagger_{j,\sigma} d_{j,\sigma} + U \sum_j n_{j,\uparrow} n_{j,\downarrow} + \vec{h} \sum_j \vec{S}_j + \frac{t}{2} \sum_\sigma \left(d^\dagger_{1,\sigma} d_{2,\sigma} + d^\dagger_{2,\sigma} d_{1,\sigma} \right) \quad (1)$$

$$H_{\rm I} = \frac{V}{\sqrt{N}} \sum_{j\in\{1,2\}k,\sigma} c^\dagger_{k,\sigma} e^{{\rm i}kR_j} d_{j,\sigma} + {\rm h.c.}, \quad (2)$$

with $d^\dagger_{j,\sigma}$ creating an electron with spin σ and energy E_j on impurity j located at position $R_{1/2} = \pm R/2$, $n_{j,\sigma} = d^\dagger_{j,\sigma} d_{j,\sigma}$, a local magnetic field $\vec{h}$ applied to the spin $\vec{S}_j = \frac{1}{2} d^\dagger_{j,\sigma} \vec{\sigma}_{\sigma,\sigma'} d_{j,\sigma}$ of impurity j and $c^\dagger_{k,\sigma}$ creates a conduction electron. At low temperatures, the tunneling t leads to an effective antiferromagnetic exchange interaction $K \vec{S}_1 \vec{S}_2$ with $K = t^2/U$ between the impurity spins. Throughout this work, unless stated otherwise, we will consider the case $E_1 = E_2 = E = -U/2$ for simplicity such that both

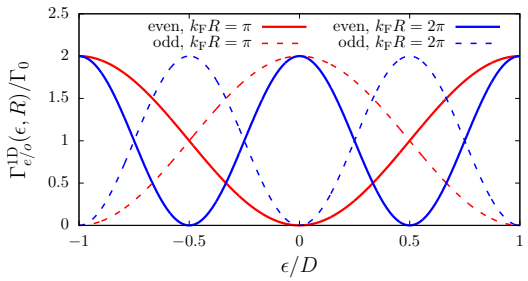

FIG. 1. Hybridization functions of Eq. (4) for a linear dispersion in 1D for two different distances $k_F R = \pi$ (red) and $k_F R = 2\pi$ (blue). For these differences either the even (solid) or the odd (dashed) hybridization function exhibit a pseudogap leading to a breakdown of the Kondo effect of the associated conduction band.

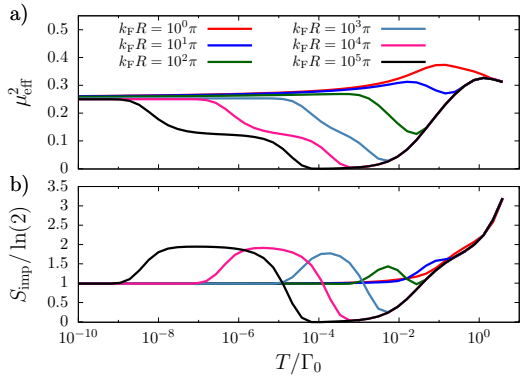

FIG. 2. (a) The effective local magnetic moment $\mu^2_{\rm eff}$ and (b) entropy of the impurities for the TIAM plotted against the temperature T for different distances.

impurities are occupied with one electron. Below, we will show that the QCP is wholly robust to departure from parity and particle-hole symmetries.

For the numerical renormalization group (NRG) approach [31–34], it is useful to introduce a parity eigenbasis $d_{e/o,\sigma} = \frac{1}{\sqrt{2}}(d_{1,\sigma} \pm d_{2,\sigma})$ for the impurity degrees of freedom [6, 14, 15, 35–38]. In this basis the states with even/odd parity couple to corresponding even/odd parity conduction bands via the energy and distance dependent hybridization functions

$$\Gamma_e(\epsilon, \vec{R}) = \frac{2\pi V^2}{N} \sum_{\vec{k}} \delta(\epsilon - \epsilon(\vec{k})) \cos^2\left(\frac{\vec{k}\vec{R}}{2}\right) \tag{3a}$$

$$\Gamma_o(\epsilon, \vec{R}) = \frac{2\pi V^2}{N} \sum_{\vec{k}} \delta(\epsilon - \epsilon(\vec{k})) \sin^2\left(\frac{\vec{k}\vec{R}}{2}\right). \tag{3b}$$

A proper consideration of the energy dependence of these functions generally breaks particle-hole symmetry [15, 16] and hence destroys the well-known QCP predicted by Jones and Varma [14, 36].

Hybridization functions.– Examining the definitions of the hybridization functions $\Gamma_{e/o}(\epsilon, \vec{R})$ reveals an important fundamental property: If all wave vectors $\vec{k}'$ fulfilling $\epsilon(\vec{k}') = 0$ also satisfy the condition $\vec{k}'\vec{R}_n = \pi n$, with n being an integer, one of the two hybridization function exhibit a pseudogap $\propto |\epsilon|^2$ because either the sine or the cosine in Eqs (3) vanishes for $\epsilon \to 0$. While for a general dispersion this requirement is not fulfilled, infinitely many equidistant $R_n = |\vec{R}_n|$ obeying this requirement are found for a 1D inversion symmetric dispersion with $\epsilon(k) = \epsilon(|k|)$.

Since the Kondo screening breaks down for a pseudogap hybridization function vanishing as $|\epsilon|^r$, with $r > 1/2$ [39–42], the Kondo effect of the even or odd conduction band will disappear for the specific distances $k' R_n = \pi n$ leading to an underscreened spin-1 Kondo fixed point (USK FP) with an effective free spin-1/2 remaining.
For a 1D linear dispersion $\epsilon(k) = v_F(|k| - k_F)$, Eqs. (3) yields [37, 38]

$$\Gamma^{1D}_{e/o}(\epsilon, R) = \Gamma_0 \left(1 \pm \cos\left[k_F R(1 + \frac{\epsilon}{D})\right]\right) \tag{4}$$

with $\Gamma_0 = \pi\rho_0 V^2$, the half bandwidth D, the constant density of states of the original conduction band $\rho_0 = 1/2D$, $k_F = \pi/2a$, and a being the lattice constant. $\Gamma^{1D}_{e/o}(\epsilon, R)$ are depicted in Fig. 1 for two different distances $k_F R = \pi, 2\pi$. The hybridization function of the even conduction band exhibits a gap for distances $k_F R = (2n+1)\pi$ and the one of the odd band for $k_F R = 2n\pi$. Note that with increasing distance R the frequency of the oscillations in $\Gamma^{1D}_{e/o}(\epsilon, R)$ increases and consequently the width of the gap becomes smaller so that the stable low energy FP is reached at increasingly lower temperatures.

Doublet ground state.– Generically, a singlet ground state is found in the TIAM since either the two impurity spins are bound in a local singlet for strong antiferromagnetic correlations between the impurities or the impurity spins are screened by the surrounding conduction band electrons to spatially extended Kondo singlets [14, 36]. A different situation arises for the specific distances $k_F R_n = n\pi$ where one conduction band decouples at low energies. This is demonstrated in Fig. 2 where the effective impurity magnetic moment $\mu^2_{\rm eff}$ and the entropy $S_{\rm imp}$ [43][31, 34] is plotted for different R_n. The USK FP with a free unquenched spin-1/2 remaining is the only stable stable fixed point for vanishing spin-spin interaction $K = 0$ ($t = 0$) characterized by $\mu^2_{\rm eff} = 0.25$ and the impurity entropy $S_{\rm imp} = \ln(2)$.

At very large distances R_n the gap in one of the hybridization functions becomes very narrow so that the crossover to the USK FP only occurs at very low temperatures. For such distances at first both impurities are screened by the two conduction bands leading to an almost vanishing magnetic moment $\mu^2_{\rm eff} \approx 0$ and entropy $S \approx 0$. However, the renormalization of the effective Kondo coupling and consequently the screening of one

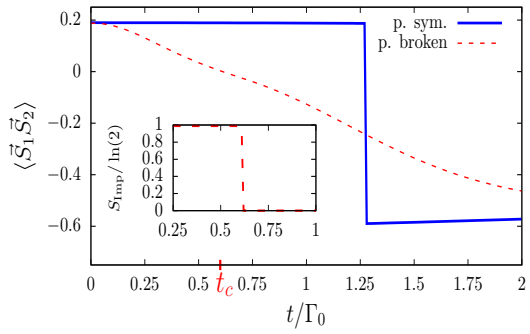

FIG. 3. The correlation function $\langle \vec{S}_1 \vec{S}_2 \rangle$ plotted against the tunneling t. While in the parity symmetric cases (solid lines) $\langle \vec{S}_1 \vec{S}_2 \rangle$ must change discontinuously, in the parity broken case the correlation function is continuous. The inset shows the entropy for the parity broken case and the new critical $t_c(\Delta E)$ is marked on the x-axis.

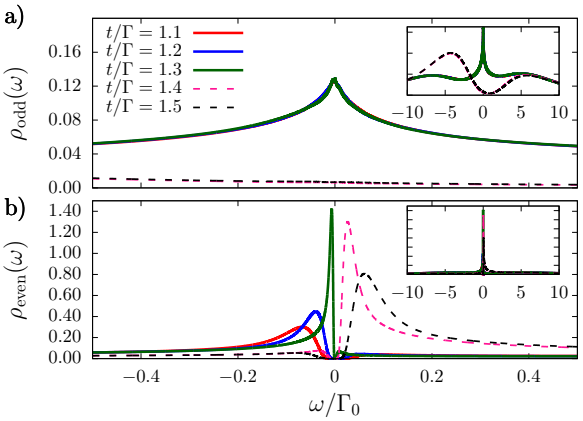

FIG. 4. Spectral function of the (a) odd and (b) even orbital for tunnelings $t < t_c$ (solid lines) and $t > t_c$ (dashed lines) and $\Delta E = 0$. For the distance $k_{\rm F}R = \pi$ the even orbital decouples at low temperatures $T \to 0$ from the conduction band.

local spin always stops at a finite temperature due to the pseudogap hybridization function and, therefore, the screening is never complete. Since the hybridization to one conduction band vanishes at the Fermi energy, the coupling to that band subsequently decreases until finally the USK FP emerges at very low temperatures.

In between these two FPs the model exhibits another unstable FP with $\mu^2_{\rm eff} = 0.125$ and entropy $S_{\rm Imp} = 2\ln(2)$. The values for $\mu^2_{\rm eff}$ and S are a feature of the the gapped Wilson chain [44] and are not related to the impurity physics. While $\mu^2_{\rm eff}(T)$ starts to increase until it reaches the value $\mu^2_{\rm eff} = 0.125$ in the regime of the unstable FP, the impurity spins remain screened so that the local moment of the impurities $\mu^2_{\rm loc}(T) = T \lim_{h_z \to 0} \langle S^z_j \rangle / h_z$ [40, 45] continues to decrease linearly with decreasing T. Since the impurity spins are only completely screened at $T = 0$ in the conventional Kondo problem, the screening of the impurity spins progresses until the USK FP is reached at low temperatures where the local moment $\mu^2_{\rm loc}(T)$ and remains constant for $T \to 0$ as it is expected for a free but strongly reduced magnetic moment in the Curie-Weiss law.

The low temperature crossover scale from the unstable FP to the stable USK FP depends on degree of screening: the smaller $\mu^2_{\rm loc}(T_{\rm Gap})$ at the energy scale $T_{\rm Gap}$ at which the pseodogap develops, the smaller the crossover temperature scale. Such a vigorous screening can be achieved in two ways: either the distance R_n is increased so that the screening stops at lower temperatures (shown in Fig. 2) or the coupling V to the bands is increased so that the impurities are already strongly screened at higher temperatures.

Quantum critical point.– While for a vanishing spin-spin interaction between the impurities the ground state is always a doublet at R_n, both impurity spins form a local spin-singlet for sufficient strong antiferromagnetic interactions K. Therefore, these two phases must be separated by a QCP. Unlike the unstable QCP of Jones and Varma [14, 15] separating two singlet ground states, this QCP is topologically protected due to the orthogonality of the two ground states. While the Jones and Varma QPT is a continuous [14, 15], the QPT discussed here is of Kosterlitz-Thouless type [46].

The different nature of the QPTs is also revealed in the local spin-spin correlation function $\langle \vec{S}_1 \vec{S}_2 \rangle$. While in the absence of K ($t = 0$) a local triplet screened by the Kondo effect at low T to a doublet is part of the ground state, a local singlet forms and suppresses the Kondo effect [14] for large antiferromagnetic K. This leads to $\langle \vec{S}_1 \vec{S}_2 \rangle \approx 1/4$ in the former regime, while in the later one finds $\langle \vec{S}_1 \vec{S}_2 \rangle \to -3/4$. For the Jones/Varma QCP, $\langle \vec{S}_1 \vec{S}_2 \rangle$ varies continuously across the QPT and only its derivative diverges at the QCP. This is due to a mixing term in the Hamiltonian [13, 14] exchanging even and odd conduction electrons via impurity scattering processes. Global parity remains conserved but local parity on the impurity subsystem is broken. This is contrasted by the behavior of $\langle \vec{S}_1 \vec{S}_2 \rangle$ at R_n as shown in Fig. 3. Since one of the two bands decouples at low energy scales, the band mixing term is suppressed, and a dynamical local parity conservation ensures the conservation of $\langle \vec{S}_1 \vec{S}_2 \rangle$ at low temperatures and prohibits the decay to its equilibrium value after a spin manipulation. Consequently the correlation function has to change discontinuously at the QCP for a parity symmetric model.

Furthermore, the QPT is even robust against parity breaking: We have added a small ΔE to one of the two single particle levels, i. e. $E_1 = E + \Delta E$, which is one of several ways of breaking the parity. Although the spin correlation function varies now continuously in the parity broken case, as depicted in Fig. 3, other quantities such as the magnetic moment $\mu^2_{\rm eff}$, the entropy $S_{\rm imp}$

(shown in the inset of Fig. 3) or the spectral functions still show a discontinuity at the renormalized critical tunneling $t_c(\Delta E)$ marked on the x-axis in Fig. 3.

For the parity conserving case, the spectra of the odd and even orbital [47, 48] are shown in Fig. 4 for the two different phases and the distance $k_F R = \pi$, at which the even orbital decouples from the conduction band at low energy scales. The spectral functions exhibit the same features as in the $R = 0$ case [6, 22] but with the role of even and odd spectra interchanged.

The spectrum for the odd orbital develops an underscreened Kondo peak [49] at the Fermi energy for $t < t_c$ which collapses once the tunnelling exceeds $t > t_c$. In this phase both impurity spins are bound into a local singlet.

In contrast, ρ_{even} always developes a gap around the Fermi energy for all $t \neq t_c$: the pseudogap in the even hybridization function suppresses the Kondo screening of the spin in the even orbital. Furthermore, at low frequencies, the orbital decouples from the hybridization processes. Injecting/ejecting an electron into/from the even orbital changes the local particle number which cannot relax but induces a suddenly changed Coulomb potential for the odd orbital. The only way the system can respond at $T = 0$ is by changing the many-body ground state. This leads to the well understood x-ray edge physics [50] also found in the Falicov-Kimball model [51]. The excitations around the Fermi energy thus indicate transitions from the doublet to the singlet phase for $t < t_c$ and vice versa for $t > t_c$. Consequently, the width of the gap in the spectrum is given by the energy difference between the doublet and singlet state and vanishes for $t \to t_c$. Note that for distances $k_F R = 2n\pi$, the spectral functions of the even and odd are interchanged.

In the general parity-broken case features of the even orbital are weakly mixed into the spectral function of the odd orbital and vice versa since in this case both orbitals are coupled to both conduction bands [6]. Experimentally the QPT can be detected by measuring the differential conductance though an impurity which is proportional to a superposition of the even and odd spectral functions. We predict that for $t < t_c$ a clear Kondo peak at the Fermi energy is visible below the Kondo temperature T_K. This Kondo peak disappears for $t > t_c$, and only the finite frequency excitations stemming from the x-ray edge physics of the weakly coupled orbital are mixed in as recently detected in a molecular dimer system[6].

Since the tunneling t is generated by the overlap of orbital wave functions of the adatoms or molecules in experiment [6], variation of the tunneling t is experimentally difficult. The case of a fixed E but different discrete t changed via molecule geometry has been recently realized [6] for the extrem case of $R \approx 0$ but is not suitable for electronic switching of the local spin configuration.

However, it is also possible to evoke the QPT for a finite fixed tunneling t via a gate voltage shifting both orbital level energies E. Figure 5 depicts the correlation function $\langle \vec{S}_1 \vec{S}_2 \rangle$ plotted against E for the two distances $k_F R = 0, \pi$ (dashed/solid lines) and various fixed tunnelings t. The discontinuous jumps in $\langle \vec{S}_1 \vec{S}_2 \rangle$ indicate the tunneling dependent critical level energy $E_c(t)$ at which the QPT occurs. For $t = \pm\Gamma_0$ the system is driven from the doublet to the singlet phase while for $t = 2\Gamma_0$ it is vice versa. The closer the tunneling is to the critical value $t_c(E)$ for a specific level energy E, the smaller is the shift in the level energies required to tune the system across the QPT. Whether a positive or negative gate voltage is needed to evoke the QPT depends on the sign of the tunneling t and the distance R_n defining which orbital decouples.

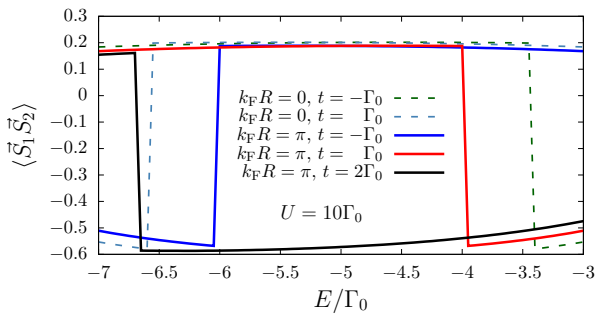

FIG. 5. $\langle \vec{S}_1 \vec{S}_2 \rangle$ plotted against E/Γ_0 for $U = 10\Gamma_0$, the two different distances $k_F R = 0, \pi$ (dashed/solid lines) and various t/Γ_0. $E = -5\Gamma_0$ is the p-h-symmetric case. The QPT can also be evoked by varying E via a gate voltage applied to the impurities.

Summary.– We have shown that the TIAM exhibit a QCP for a 1D dispersion $\epsilon(k) = \epsilon(|k|)$ in the cases that the impurities are separated by specific distances R_n. In contrast to the unstable QCP [14] usually discussed in the context of the two impurity models, the QCP presented in this Letter is stable to departure from particle-hole and parity symmetry. The pseudogap in one parity channel leads to an underscreened Kondo effect with a doublet ground state which is topological different to the singlet ground state for large antiferromagnetic interactions between the impurity spins.

Although a small departure from the specific distances theoretically always leads to a singlet ground state at very low temperatures, the system will stay in the now unstable doublet fixed point for all experimentally relevant temperatures if the departure is not to large. Calculations have shown that a variance of R_n by 15 % of the lattice constant should be still sufficient to detect a sharp change in the magnetic properties of the system at low temperatures.

We believe that this system may be of great relevance for spintronic devices since it is possible by applying gate voltages to turn on and off a free magnetic moment which is not screened at low temperatures. Along with the mag-

netic moment one can switch on and off a Kondo effect with its sharp conductance peak at the Fermi energy. Furthermore, in the parity symmetric case the spin-spin correlation between both impurity spins is protected by the parity as a conserved quantity making this system promising for spin-qubit realizations.

We acknowledge useful discussions with S. F. Tautz and R. Bulla.

[1] I. Žutić, J. Fabian, and S. Das Sarma, Rev. Mod. Phys. **76**, 323 (2004).

[2] M. Misiorny, M. Hell, and M. R. Wegewijs, Nat Phys **9**, 801 (2013).

[3] W. Han, R. K. Kawakami, M. Gmitra, and J. Fabian, Nat Nano **9**, 794 (2014).

[4] H. Johll, M. D. K. Lee, S. P. N. Ng, H. C. Kang, and E. S. Tok, Scientific Reports **4**, 7594 (2014).

[5] O. V. Yazyev and L. Helm, Phys. Rev. B **75**, 125408 (2007).

[6] T. Esat, B. Lechtenberg, T. Deilmann, C. Wagner, P. Kruger, R. Temirov, M. Rohlfing, F. B. Anders, and F. S. Tautz, Nat Phys **12**, 867 (2016).

[7] N. Atodiresei, J. Brede, P. Lazić, V. Caciuc, G. Hoffmann, R. Wiesendanger, and S. Blügel, Phys. Rev. Lett. **105**, 066601 (2010).

[8] L. Bogani and W. Wernsdorfer, Nat Mater **7**, 179 (2008).

[9] S. Sanvito, Chem. Soc. Rev. **40**, 3336 (2011).

[10] W. J. M. Naber, S. Faez, and W. G. van der Wiel, Journal of Physics D: Applied Physics **40**, R205 (2007).

[11] V. A. Dediu, L. E. Hueso, I. Bergenti, and C. Taliani, Nat Mater **8**, 707 (2009).

[12] A. J. Drew, J. Hoppler, L. Schulz, F. L. Pratt, P. Desai, P. Shakya, T. Kreouzis, W. P. Gillin, A. Suter, N. A. Morley, V. K. Malik, A. Dubroka, K. W. Kim, H. Bouyanfif, F. Bourqui, C. Bernhard, R. Scheuermann, G. J. Nieuwenhuys, T. Prokscha, and E. Morenzoni, Nat Mater **8**, 109 (2009).

[13] O. Sakai and Y. Shimizu, Journal of the Physical Society of Japan **61**, 2333 (1992), http://dx.doi.org/10.1143/JPSJ.61.2333.

[14] B. A. Jones, C. M. Varma, and J. W. Wilkins, Phys. Rev. Lett. **61**, 125 (1988); B. A. Jones and C. M. Varma, Phys. Rev. B **40**, 324 (1989).

[15] I. Affleck, A. W. W. Ludwig, and B. A. Jones, Phys. Rev. B **52**, 9528 (1995).

[16] R. M. Fye, Phys. Rev. Lett. **72**, 916 (1994).

[17] R. M. Fye, J. E. Hirsch, and D. J. Scalapino, Phys. Rev. B **35**, 4901 (1987); R. M. Fye and J. E. Hirsch, Phys. Rev. B **40**, 4780 (1989).

[18] J. B. Silva, W. L. C. Lima, W. C. Oliveira, J. L. N. Mello, L. N. Oliveira, and J. W. Wilkins, Phys. Rev. Lett. **76**, 275 (1996).

[19] L. Zhu and C. M. Varma, eprint arXiv:cond-mat/0607426 (2006), cond-mat/0607426.

[20] The USK FP differs from the strong coupling fixed point usually discussed in the context of an underscreened Kondo effect by an additional free conduction band with zero phase shift.

[21] M. Vojta, R. Bulla, and W. Hofstetter, Phys. Rev. B **65**, 140405 (2002).

[22] S. Nishimoto, T. Pruschke, and R. M. Noack, Journal of Physics: Condensed Matter **18**, 981 (2006).

[23] M. A. Blachly and N. Giordano, Phys. Rev. B **46**, 2951 (1992).

[24] J. F. DiTusa, K. Lin, M. Park, M. S. Isaacson, and J. M. Parpia, Phys. Rev. Lett. **68**, 678 (1992).

[25] M. A. Blachly and N. Giordano, Phys. Rev. B **51**, 12537 (1995).

[26] P. Mohanty and R. A. Webb, Phys. Rev. Lett. **84**, 4481 (2000).

[27] H. Masai, J. Terao, S. Seki, S. Nakashima, M. Kiguchi, K. Okoshi, T. Fujihara, and Y. Tsuji, .

[28] A. V. Gorshkov, M. Hermele, V. Gurarie, C. Xu, P. S. Julienne, J. Ye, P. Zoller, E. Demler, M. D. Lukin, and A. M. Rey, Nat Phys **6**, 289 (2010).

[29] L.-M. Duan, Europhys. Lett. **67**, 721 (2004).

[30] B. Paredes, C. Tejedor, and J. I. Cirac, Phys. Rev. A **71**, 063608 (2005).

[31] K. G. Wilson, Rev. Mod. Phys. **47**, 773 (1975).

[32] H. R. Krishna-murthy, J. W. Wilkins, and K. G. Wilson, Phys. Rev. B **21**, 1003 (1980).

[33] H. R. Krishna-murthy, J. W. Wilkins, and K. G. Wilson, Phys. Rev. B **21**, 1044 (1980).

[34] R. Bulla, T. A. Costi, and T. Pruschke, Rev. Mod. Phys. **80**, 395 (2008).

[35] C. Jayaprakash, H. R. Krishna-murthy, and J. W. Wilkins, Phys. Rev. Lett. **47**, 737 (1981).

[36] B. A. Jones and C. M. Varma, Phys. Rev. Lett. **58**, 843 (1987).

[37] L. Borda, Phys. Rev. B **75**, 041307 (2007).

[38] B. Lechtenberg and F. B. Anders, Phys. Rev. B **90**, 045117 (2014).

[39] R. Bulla, T. Pruschke, and A. C. Hewson, Journal of Physics: Condensed Matter **9**, 10463 (1997).

[40] C. Gonzalez-Buxton and K. Ingersent, Phys. Rev. B **57**, 14254 (1998).

[41] K. Chen and C. Jayaprakash, Journal of Physics: Condensed Matter **7**, L491 (1995).

[42] K. Ingersent, Phys. Rev. B **54**, 11936 (1996).

[43] Both quantities $\mu^2_{\rm eff}$ and $S_{\rm imp}$ are calculated as usual in the NRG via $A(T) = A_{\rm tot}(T) - A_{\rm free}(T)$ where $A_{\rm tot}(T)$ is the measured quantity of the total system, consisting of the impurities coupled to the bath. From this, the quantity of a reference system, i.e., one without impurities is subtracted.

[44] More details on the origin of this unstable fixed point can be found in the supplement.

[45] T. Chowdhury and K. Ingersent, Phys. Rev. B **91**, 035118 (2015).

[46] W. Hofstetter and H. Schoeller, Phys. Rev. Lett. **88**, 016803 (2001).

[47] R. Peters, T. Pruschke, and F. B. Anders, Phys. Rev. B **74**, 245114 (2006).

[48] A. Weichselbaum and J. von Delft, Phys. Rev. Lett. **99**, 076402 (2007).

[49] N. Roch, S. Florens, T. A. Costi, W. Wernsdorfer, and F. Balestro, Phys. Rev. Lett. **103**, 197202 (2009).

[50] B. Roulet, J. Gavoret, and Nozières, Phys. Rev. **178**, 1072 (1969); N. P. and C. T. de Dominicis, *ibid.* **178**, 1097 (1969).

[51] Q. Si, G. Kotliar, and A. Georges, Phys. Rev. B **46**, 1261 (1992); F. B. Anders and G. Czycholl, Phys. Rev. B **71**, 125101 (2005).

Supplementary Material

MAPPING TO THE PARITY BASIS

While Wilsons original numerical renormalization group (NRG) approach was only designed to solve the thermodynamics of one localized impurity, the NRG was later successfully extended by Jones and Varma [1–7] to two impurities which were separated by a distance R. The conduction band is divided into two conduction bands, one with even and one with odd parity symmetry, whose effective densities of states (DOSs) incorporated the spatial extension. In the following, we briefly summarize this procedure for the two impurity Anderson model (TIAM).

The Hamiltonian of the TIAM can be separated into three parts $H = H_\mathrm{c}+H_\mathrm{D}+H_\mathrm{I}$. H_c contains the conduction band $H_c = \sum_{\vec{k},\sigma} \epsilon_{\vec{k}} c^\dagger_{\vec{k},\sigma} c_{\vec{k},\sigma}$ where $c^\dagger_{\vec{k},\sigma}$ creates an electron with spin σ and momentum $\vec{k}$. H_D comprises the contribution of the impurities

$$H_d = \sum_{j,\sigma} E_j d^\dagger_{j,\sigma} d_{j,\sigma} + U \sum_j n_{j,\uparrow} n_{j,\downarrow} + \frac{t}{2} \sum_\sigma \left(d^\dagger_{1,\sigma} d_{2,\sigma} + d^\dagger_{2,\sigma} d_{1,\sigma} \right), \tag{S1}$$

with $d^\dagger_{j,\sigma}$ creating an electron on impurity j with the level energy E_j, $n_{j,\sigma} = d^\dagger_{j,\sigma} d_{j,\sigma}$, the Coulomb repulsion U and a tunneling t between the impurities. The interaction between the conduction band and the impurities is given by

$$H_\mathrm{I} = \frac{V}{\sqrt{N}} \sum_{j\in\{1,2\}k,\sigma} c^\dagger_{\vec{k},\sigma} e^{\mathrm{i}\vec{k}\vec{R}_j} d_{j,\sigma} + \mathrm{h.c.}, \tag{S2}$$

where V is the hybridization strength between the conduction band and the two impurities which are located at $\vec{R}_{1/2} = \pm\frac{\vec{R}}{2}$. For simplicity we will consider the case particle-hole and parity symmetric case $E_1 = E_2 = -U/2$.

For the NRG, it is useful [1–8] to include spatial dependency into the two orthogonal energy-dependent even (e) and odd (o) parity eigenstate field operators

$$c_{\epsilon,\sigma,e/o} = \sum_{\vec{k}} \delta(\epsilon - \epsilon_{\vec{k}}) c_{\vec{k}\sigma} \frac{\left(e^{+i\vec{k}\vec{R}/2} \pm e^{-i\vec{k}\vec{R}/2} \right)}{N_{e/o}(\epsilon, \vec{R}) \sqrt{N \rho_c(\epsilon)}}. \tag{S3}$$

Here $\rho_c(\epsilon)$ is the density of states (DOS) of the conduction band and the dimensionless normalization functions are defined as

$$N^2_e(\epsilon, \vec{R}) = \frac{4}{N\rho_c(\epsilon)} \sum_{\vec{k}} \delta(\epsilon - \epsilon_{\vec{k}}) \cos^2\left(\frac{\vec{k}\vec{R}}{2}\right) \tag{S4a}$$

$$N^2_o(\epsilon, \vec{R}) = \frac{4}{N\rho_c(\epsilon)} \sum_{\vec{k}} \delta(\epsilon - \epsilon_{\vec{k}}) \sin^2\left(\frac{\vec{k}\vec{R}}{2}\right). \tag{S4b}$$

such that $c_{\epsilon,\sigma,e/o}$ fulfill the standard anticommutator relation $\{c_{\epsilon,\sigma,p}, c^\dagger_{\epsilon',\sigma',p'}\} = \delta_{\sigma,\sigma'}\delta_{p,p'}\delta(\epsilon-\epsilon')$. If we also introduce even and odd parity combinations for the orbitals

$$d_{e/o,\sigma} = \frac{1}{\sqrt{2}} \left(d_{1,\sigma} \pm d_{2,\sigma} \right) \tag{S5}$$

H_D and H_I are given by

$$H_\mathrm{I} = \sum_{p=\{e,o\},\sigma} E_p d^\dagger_{p,\sigma} d_{p,\sigma} + \frac{U}{2} \sum_p n_{p,\uparrow} n_{p,\downarrow} + \frac{U}{4} \sum_{\sigma,\sigma'} n_{e,\sigma} n_{o,\sigma'} - U \vec{S}_e \vec{S}_o + \frac{U}{2} \left(d^\dagger_{e,\uparrow} d^\dagger_{e,\downarrow} d_{o,\downarrow} d_{o,\uparrow} + \mathrm{h.c.} \right) \tag{S6}$$

$$H_\mathrm{I} = \frac{V}{\sqrt{2}} \sum_\sigma \int d\epsilon \sqrt{\rho_c(\epsilon)} \left\{ N_e(\epsilon, \vec{R}) c^\dagger_{e,\sigma}(\epsilon) d_{e,\sigma} + N_o(\epsilon, \vec{R}) c^\dagger_{o,\sigma}(\epsilon) d_{o,\sigma} + \mathrm{h.c.} \right\} \tag{S7}$$

$$= \sum_\sigma \left\{ \sqrt{\frac{\Gamma_e(\epsilon, R)}{\pi}} c^\dagger_{e,\sigma}(\epsilon) d_{e,\sigma} + \sqrt{\frac{\Gamma_o(\epsilon, R)}{\pi}} c^\dagger_{o,\sigma}(\epsilon) d_{o,\sigma} + \mathrm{h.c.} \right\}. \tag{S8}$$

Here we defined the local spin operator $\vec{S}_{e/o} = \frac{1}{2} \sum_{\alpha,\beta} d^\dagger_{e/o,\alpha} \vec{\sigma}_{\alpha,\beta} d_{e/o,\alpha}$ with $\vec{\sigma}$ being Pauli matrices, and the even and odd energy level is given by $E_{e/o} = E \pm t/2$. The hybridization functions in (S8) are defined as $\Gamma_{e/o}(\epsilon, R) = \pi V^2 \rho_c(\epsilon) \frac{N^2_{e/o}(\epsilon,\vec{R})}{2}$.

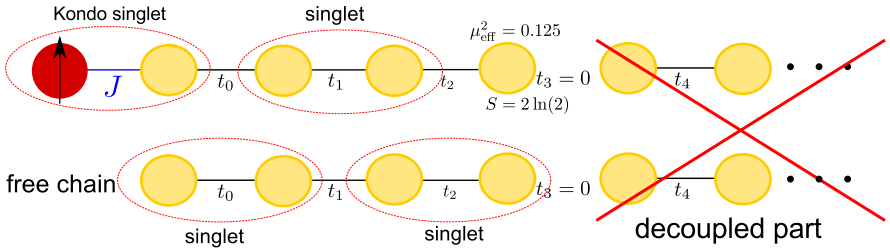

FIG. S1. Schematic view of the gapped Wilson chain (top) with the impurity coupled to it and (bottom) without the impurity. The values $\mu^2_{\rm eff} = 0.125$ for the magnetic moment and $S = 2\ln(2)$ for the entropy compared to the free chain are caused by the by a Wilson site which is not bound into a singlet.

DISCONTINUITY IN THE CORRELATION FUNCTION $\langle \vec{S}_1 \vec{S}_2 \rangle$

In order to understand the properties of the topologically protected QCP and its differences to the previous known QCP [2–4, 9] it is useful to consider the effective low temperature Hamiltonian for the large U limit. Via a Schrieffer-Wolff transformation [10, 11] one obtains the two impurity Kondo model (TIKM) [1–4]

$$H_{\rm K,I} = \frac{J}{8} \int\int d\epsilon\, d\epsilon' \sqrt{\rho_c(\epsilon)\rho_c(\epsilon')} \sum_{p,\sigma\sigma'} \vec{\sigma}_{\sigma\sigma'} \Big[(\vec{S}_1 + \vec{S}_2) \left(N_p(\epsilon,R) N_p(\epsilon',R) c^\dagger_{\epsilon\sigma,p} c_{\epsilon'\sigma',p} \right) + (\vec{S}_1 - \vec{S}_2) N_e(\epsilon,R) N_o(\epsilon',R) \left(c^\dagger_{\epsilon\sigma,e} c_{\epsilon'\sigma',o} + \text{h.c.} \right) \Big] \tag{S9a}$$

$$H_{K,D} = K \vec{S}_1 \vec{S}_2. \tag{S9b}$$

with $J = \frac{8V^2}{U}$ and $K = \frac{t^2}{U}$.

At low temperature the last term of Eq. (S9a) proportional to $(\vec{S}_1 - \vec{S}_2)$ always vanishes since either $N_e(\epsilon, R) \to 0$ or $N_o(\epsilon, R) \to 0$ for $\epsilon \to 0$. This term transfers "parity" from the impurity to the conduction band, therefore, $\langle \vec{S}_1 \vec{S}_2 \rangle$ may change continuously from a triplet with parity $+1$ to a singlet with parity -1 as long as this term is present. However, since this term disappears at low energy scales, the correlation function has to change discontinuously at the QCP for a parity symmetric model. This discontinuity is hence a consequence of parity conservation.

UNSTABLE INTERMEDIATE FIXED POINT

To reveal that the unstable intermediate fixed point is just a feature of the Wilson chain for a pseudogap DOS we recall that impurity contributions are computed with the numerical renormalization group (NRG) by calculating a quantity for the whole system, consisting of the impurity coupled to the bath, and subtracting the quantity of the system without impurity from it

$$A(T) = A_{\rm tot}(T) - A_{\rm free}(T) \tag{S10}$$

where $A_{\rm tot}(T)$ is the measured quantity of the whole system and $A_{\rm free}(T)$ the one without impurity.

The pseudogap in $\Gamma_{e/o}(\epsilon, R)$ leads to a characteristic features of the tight-binding matrixelements t_n of the Wilson chain: at the energy scale $E_m \propto D\Lambda^{-m/2}$, corresponding to the energy scale $E_{\rm gap}$ at which the pseudogap starts to develop, the matrixelement t_m is strongly reduced, and for $n > m$, the matrixelements t_n alternate in magnitude. Since a fermionic DOS has negative and positive energy contributions, m must be odd. The t_n for even n are large forming a binding (negative energy) and anti-binding orbital representing the energy scale $E_n \propto D\Lambda^{-n/2}$ which are only weakly connected to orbitals of neigboring energy shells, i. e. t_n is small for odd n.

In Fig. S1, a schematic view of the gapped Wilson chain (top) with the impurity coupled to it and (bottom) without impurity is shown. For clarity, we artificially set $t_m = 0$ – here depicted for $m = 3$ – and disconnect the rest of the chain from the problem. Furthermore, we consider the strong coupling limit $J \to \infty$ for a single band $s - 1/2$ Kondo model. This decoupled part is identical for the whole system and the free chain. Since it decouples from the problem for $t_m = 0$, these degrees of freedom do not contribute to Eq. (S10).

At each NRG iteration all eigenenergies are rescaled by a factor $\sqrt{\Lambda}$, with Λ being the discretization parameter of the NRG. Therefore, high energy states of the first part are renormalized to ∞ so that only the groundstate of the first part of the Wilson chain for the iteration $N = m$ remains.

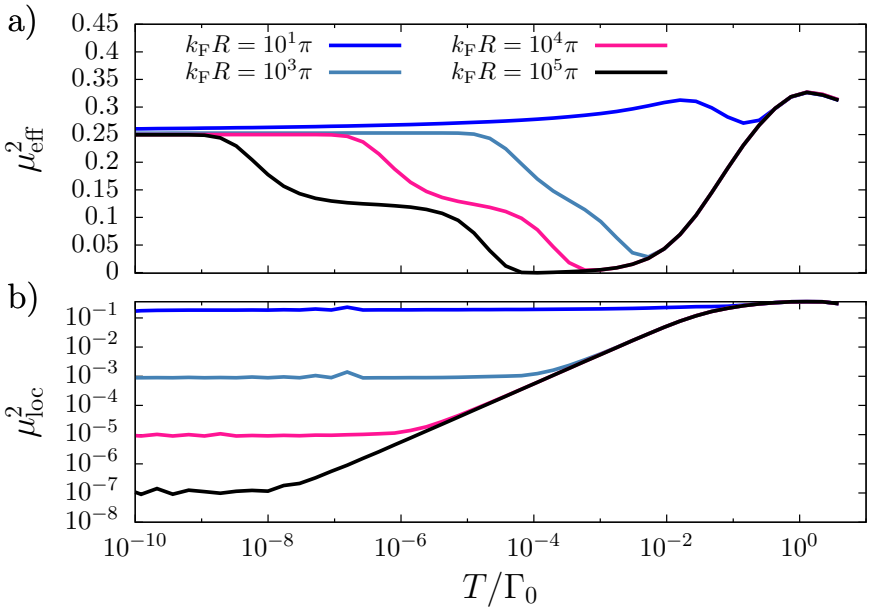

FIG. S2. (a) Effective local magnetic moment $\mu^2_{\rm eff}$ and (b) the local moment of an impurity $\mu^2_{\rm loc}$ calculated by applying a small magnetic field $h_z = 10^{-10}\Gamma_0$ to the impurity spin. In contrast to $\mu^2_{\rm eff}$ the impurity local moment $\mu^2_{\rm loc}$ shows no intermediate unstable fixed point.

This groundstate is a singlet, however, the chain with impurity has one Wilson site that is not bound into a singlet, cf. Fig. S1. For a particle-hole symmetric pseudogap DOS, the last site contributes a free orbital, leading to an effective magnetic moment of $\mu^2_{\rm eff} = 0.125$ and a entropy $S_{\rm imp} = 2\ln(2)$ employing the definition (S10). Therefore, the values for the magnetic moment and entropy at the unstable FP (Fig. 2 in the Letter) are essentially contributions from the Wilson chain for a pseudogap DOS. This also illustrates, that the effective free moment of the stable FP is generated mainly from the conduction electron degrees of freedom.

The groundstate of the first part, however, is almost degenerated with other excited states depending on the effective renormalized Kondo coupling J. The larger the renormalized coupling J the smaller the energy difference between the groundstate and those excited states. This energy difference defines the energy scale at which the transition to the USK FP occurs so that the apparent degeneracy is lifted due to the rescaling of the energies and the system flows to the stable USK FP.

LOCAL MOMENT OF THE IMPURITY $\mu^2_{\rm loc}$

As discussed in the Letter, the effective local magnetic moment $\mu^2_{\rm eff}(t)$, depicted in Fig. S2a, reveals an intermediate unstable FP caused by the Wilson chain for a pseudogap DOS. The value of $\mu^2_{\rm eff} = 0.125$ is generated by the conduction band based on the mechanism discussed in the previous section.

In contrary to $\mu^2_{\rm eff}(T)$, the local response $\mu^2_{\rm loc}(T) = T\lim_{h_z\to 0}\langle S^z_j\rangle/h_z$ demonstrate that the impurity spins remain screened [12, 13] which can be seen in Fig. S2(b).

While $\mu^2_{\rm eff}(T)$ starts to increase for decreasing temperatures corresponding to the energy scale at which the gap occurs until it reaches the value $\mu^2_{\rm eff} = 0.125$ in the regime of the unstable fixed point, the impurity spins are continued to be screened, and the local moment of the impurities $\mu^2_{\rm loc}(T)$ decrease linearly with decreasing T, since the local susceptibility $\chi_{\rm loc} = \lim_{h_z\to 0}\langle S^z_j\rangle/h_z$ has reached a constant value and shows the behavior of a Pauli-susceptibility characteristic for a Kondo screened impurity. The screening of the impurity spins progresses until the underscreened Kondo fixed point (USK FP) point is reached at low temperatures, because the impurity spins are only completely screened at $T = 0$ in the conventional Kondo problem. There, the effective local magnetic moment takes the value $\mu^2_{\rm eff} = 0.25$ and $\mu^2_{\rm loc}(T)$ reaches a very small but finite value corresponding to a Curie-Weiss behavior of a free but strongly reduced magnetic moment. $\mu^2_{\rm loc}(T)$ is a monotonically decreasing function with decreasing temperature until the USK FP is reached as shown in Fig. S2(b). Since $\mu^2_{\rm eff}(T)/\mu^2_{\rm loc}(T) = {\rm const}$ at the stable FP, there is very small but finite overlap between the local magnetic moment and the free effective spin at the FP.

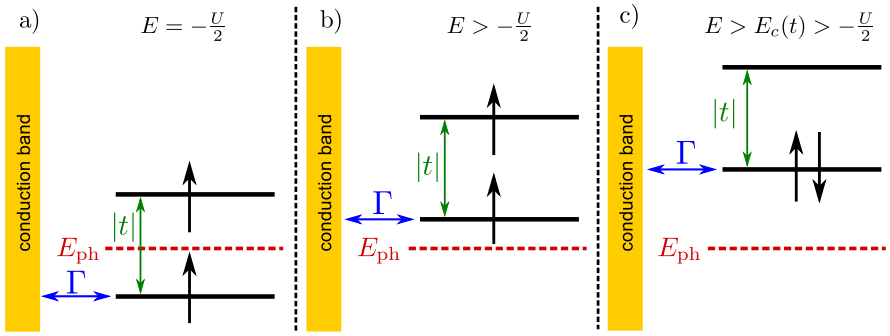

FIG. S3. Schematic view of the energy levels in the parity basis for (a) $E = -U/2$, (b) $E > -U/2$ and (c) $E > E_c(t) > -U/2$ for the case that the tunneling t shifts the decoupled orbital above the single particle energy E. $E_{\rm ph} = -U/2$ indicates the particle-hole symmetric energy level.

QUANTUM PHASE TRANSITION DRIVEN BY A GATE VOLTAGE

As demonstrated in Fig. 5 in the Letter, the QCP can be reached by applying a gate voltage shifting the level energies E of the impurities. Whether a positive or negative gate voltage is needed to evoke the quantum phase transition depends on the sign of the tunneling t and the distance R_n defining which orbital decouples.

To understand this behavior it is useful to monitor the single particle energies in the even/odd-parity basis where both energies are split by the tunneling $E_{e/o} = E \pm t/2$, so that one orbital is shifted above and the other below the center of gravity $E = -U/2$ schematically illustrated in Fig. S3a.

For $|t| < t_c$ a transition from the doublet to the singlet phase can now be caused by shifting the decoupled orbital even further away from the particle-hole symmetric point $E_{\rm ph} = -U/2$ via a variation of the particle energies E as depicted in Fig. S3b. Since the decoupled orbital can not be continuously depopulated, the system responds by changing to the singlet phase at a critical level energy $E_c(t)$ leading to an almost doubly occupied coupled orbital as shown in Fig. S3c. In contrast, if the decoupled orbital is shifted below E by the tunneling t, the single particle energies also have to be decreased $E < -U/2$ in order to achieve a transition to the singlet phase.

[1] B. A. Jones and C. M. Varma, Phys. Rev. Lett. **58**, 843 (1987).
[2] B. A. Jones, C. M. Varma, and J. W. Wilkins, Phys. Rev. Lett. **61**, 125 (1988).
[3] B. A. Jones and C. M. Varma, Phys. Rev. B **40**, 324 (1989).
[4] I. Affleck, A. W. W. Ludwig, and B. A. Jones, Phys. Rev. B **52**, 9528 (1995).
[5] L. Borda, Phys. Rev. B **75**, 041307 (2007).
[6] B. Lechtenberg and F. B. Anders, Phys. Rev. B **90**, 045117 (2014).
[7] T. Esat, B. Lechtenberg, T. Deilmann, C. Wagner, P. Kruger, R. Temirov, M. Rohlfing, F. B. Anders, and F. S. Tautz, Nat Phys **12**, 867 (2016).
[8] C. Jayaprakash, H. R. Krishna-murthy, and J. W. Wilkins, Phys. Rev. Lett. **47**, 737 (1981).
[9] M. R. Galpin, D. E. Logan, and H. R. Krishnamurthy, Phys. Rev. Lett. **94**, 186406 (2005).
[10] J. R. Schrieffer and P. A. Wolff, Phys. Rev. **149**, 491 (1966).
[11] R. Žitko and J. Bonča, Phys. Rev. B **74**, 045312 (2006).
[12] C. Gonzalez-Buxton and K. Ingersent, Phys. Rev. B **57**, 14254 (1998).
[13] T. Chowdhury and K. Ingersent, Phys. Rev. B **91**, 035118 (2015).